An experimental investigation of slabs, subjected to concentrated loads

Autor(en): **Kist, H.J. / Bouma, A.L.**

Objekttyp: **Article**

Zeitschrift: **IABSE publications = Mémoires AIPC = IVBH Abhandlungen**

Band (Jahr): **14 (1954)**

PDF erstellt am: **16.07.2024**

Persistenter Link: https://doi.org/10.5169/seals-13942

An Experimental Investigation of Slabs, Subjected to Concentrated Loads

Recherches expérimentales relatives aux dalles soumises à des charges concentrées

Über eine experimentelle Untersuchung an Platten, welche durch Einzellasten beansprucht werden

Prof. Ir. H. J. KIST, Professor at the Technological University Delft,
Ir. A. L. BOUMA, Research Engineer, Delft

Notations

a = l = span of the slab
h = thickness of the slab
E = Young's modulus of the material of the model
ν = Poisson's ratio of the material of the model
P = magnitude of the concentrated load
D = $2e$ = diameter of the load
e/a = concentration of the load
e' = fictive radius by load-distribution according to WESTERGAARD
p = distributed load pro m^2
x = coordinate in the direction of the span
y = coordinate perpendicular to the span
x_i = section of the slab perpendicular to the x-axis
y_i = section of the slab perpendicular to the y-axis
ϵ_x = strain in x-direction
ϵ_y = strain in y-direction
σ_x = normal stress in x-direction
σ_y = normal stress in y-direction
M_x = bending moment pro unit of length in a section perpendicular to the x-direction

M_y = bending moment pro unit of length in a section perpendicular to the y-direction
W = section-modulus of the slab
$K = \frac{E h^3}{12(1-\nu^2)}$ = flexural rigidity of the slab
w = deflection of the slab

Introduction

The problem concerned is of interest for the design of reinforced concrete bridges and also for reinforced concrete floor slabs in industrial buildings.

The first results have already been published in the Preliminary Publication of the fourth congress of the I.A.B.S.E. at Cambridge and London, in August and September 1952 on page 237—242.

To be able to compare the results of an experimental investigation with the results of the theory of elasticity, it is necessary that the properties of the material of the model conform to the assumptions on which this theory is based; this means that the material should be homogeneous, isotropic and following Hooke's law. This is the principal reason why the model has been made of steel. Moreover a steel model can be constructed on a much smaller scale than a concrete model, and also it is easier to make a great number of observations on a steel model for many different schemes of loading.

Interpreting the results of the measurements on reinforced concrete slabs, one meets the difficulty that this material does not satisfy the premises mentioned above. Therefore it will still be necessary to compare these results with the results of experiments on reinforced concrete slabs.

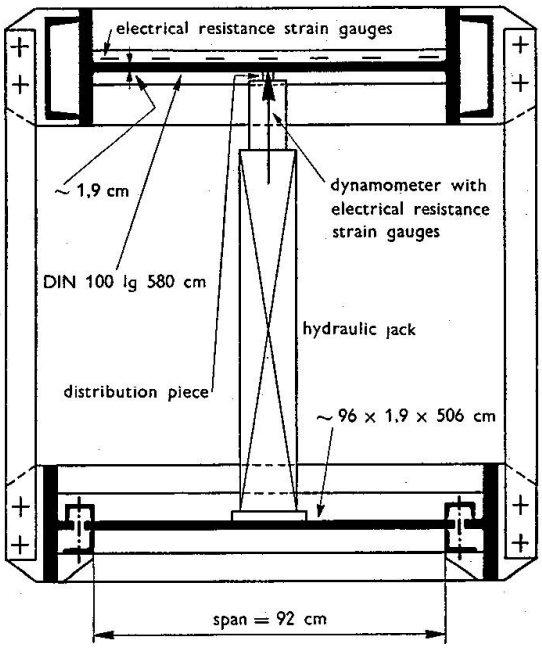

Fig. 1. Section of the model.

Description of Model and Tests

The steel model consists of two horizontal rectangular slabs of St. 37 (fig. 1 and 2). One of these slabs is the web of a beam DIN 100, with a length of 580 cm; the web has a thickness of about 1,9 cm. The torsional resistance of the flanges of the beam has considerably been increased by welding on channels. This web may be considered to be completely clamped along the long sides. The other slab, long about 506 cm and thick about 1,9 cm is simply supported along the long sides. The distance between these supports is 92 cm and is called the span.

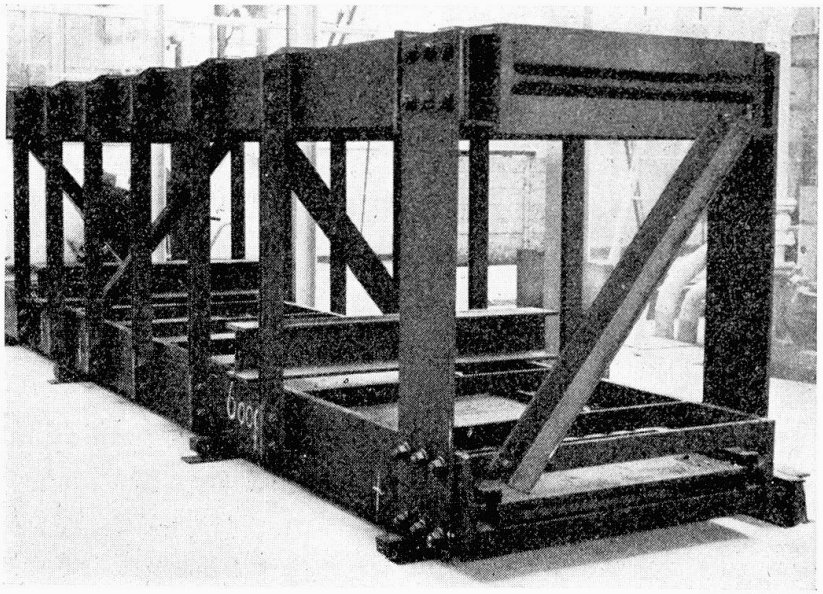

Fig. 2. The model.

The slabs are vertically united above one another by a rigid frame.

Along one short side the slabs are clamped, along the other they are simply supported. These supports could be removed in order to make these short sides entirely free.

To eliminate welding stresses the whole model has been stress-relieved.

With the model the types of boundary conditions shown in fig. 3 could be investigated.

The load was applied by a hydraulic jack, vertically placed between the slabs.

To keep the oil-pressure constant a pressure accumulator was used.

The magnitude of the load was measured with a dynamometer provided with electrical resistance strain-gauges and was kept limited to assure the validity of Hooke's law.

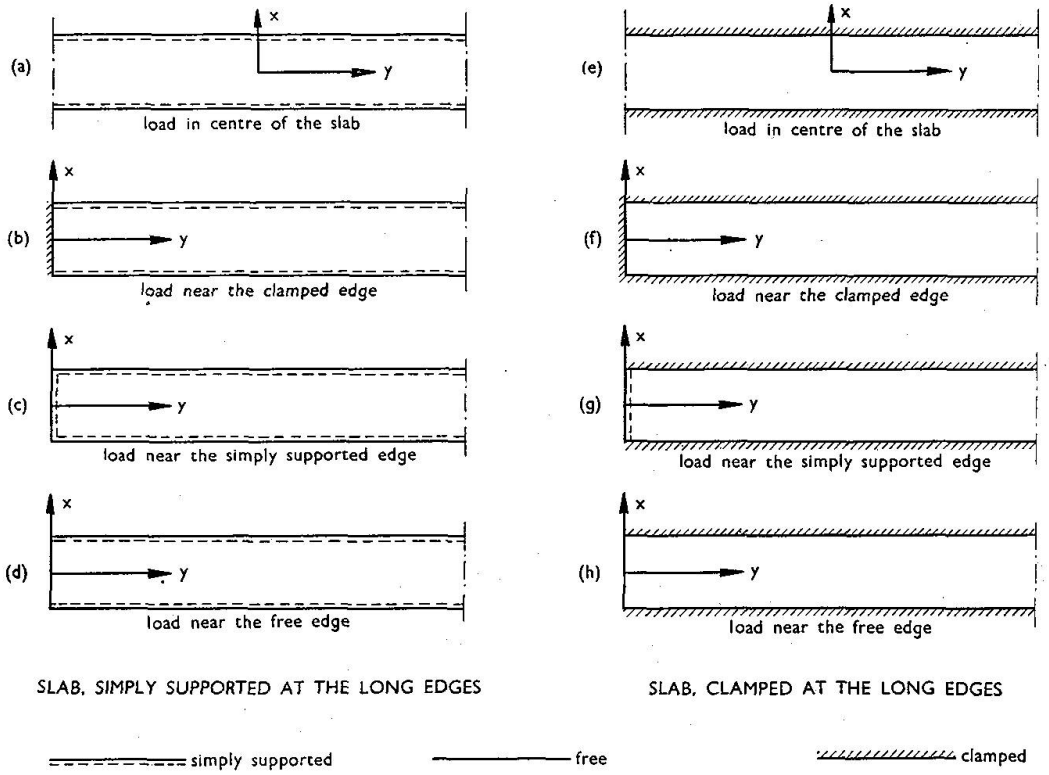

Fig. 3. The different cases of boundary conditions.

All measuring was done for a load of about 1500 kg. Preliminary measurements showed that there was a linear relation between the magnitude of the load and the measured strains.

The stresses and the bending moments in the slab were determined from the strains measured with electrical resistance strain-gauges. Their small length (generally 12 mm), the central observation, and their usefulness for a long period are here of great advantage.

To calculate the bending moment in one direction it is necessary to know the strains in this direction and the strains perpendicular to this direction. The bending moments may then be calculated from the following formulæ:

$$M_x = \sigma_x \cdot W = \frac{E}{1-\nu^2}(\epsilon_x + \nu\,\epsilon_y)\cdot\frac{1}{6}h^2$$

$$M_y = \sigma_y \cdot W = \frac{E}{1-\nu^2}(\epsilon_y + \nu\,\epsilon_x)\cdot\frac{1}{6}h^2$$

For the first measurements, on the central part of the simply supported slab, it was supposed that the supports along the short sides of the slab do not influence the stress-distribution; in other words, in this case the slab may be considered to be infinitely wide. At each measuring point the strain was only measured in one direction. By choosing a suitable scheme a value of ϵ_x at one point could always be combined with a value of ϵ_y measured at another point.

Experiments showed that it was possible to paste the strain-gauges across each other, and still get reliable results. For the following measurements this method was used and so strains perpendicular to each other were measured at the same point. In this way the measuring programm was shortened considerably.

The experimental investigation may be divided in two parts:

1. Investigation of the influence of the size of the loaded surface (the concentration of the load) on the bending moments in the slab.
2. Investigation of the stress-distribution in the slab as a function of the boundary-conditions and the location of the load.

Part 1 requires that the size of the loaded surface has to be varied. For the measurements on the central parts of the simply supported and the clamped slab the load was in succession transmitted by a ball (which gave a contact-area with a diameter of about 0,45 cm) and by circular distribution-pieces with a diameter D of 1,6 cm, 3,6 cm, 5,4 cm and 7,6 cm. The ratio's e/a (radius distribution-piece/span) were respectively 0,0024, 0,0087, 0,0195, 0,0293 and 0,0411).

For these measurements also investigations were made with various intermediate layers such as: three mm cardboard and rubber with various thicknesses. The influence of the intermediate layers proved to be very dependent on the diameter of the distribution-piece. Always the cardboard gave however the mean values. For the measurements near the short sides therefore only cardboard has been used. Near the short sides the diameter of the distribution-piece has always been $D = 1{,}6$ cm.

Part 2 requires that the load has to be placed at various points of the different parts of the slabs.

The thicknesses of the slabs have been determined at each measuring-point with a kathetometer.

Young's modulus and Poisson's ratio have been determined from a number of test bars taken from both slabs. The average values were approximately: $E = 2{,}15 \cdot 10^6$ kg/cm^2 and $\nu = 0{,}3$.

The Results

A. The central parts of the simply supported and the clamped slab (cases *a* and *e*, fig. 3)

1. The influence of the concentration on the extreme bending moments

The ratios M_x/P and M_y/P in fig. 4 are plotted as a function of the concentration (the ratio e/a) of the load, when the load is placed at various points of the span.

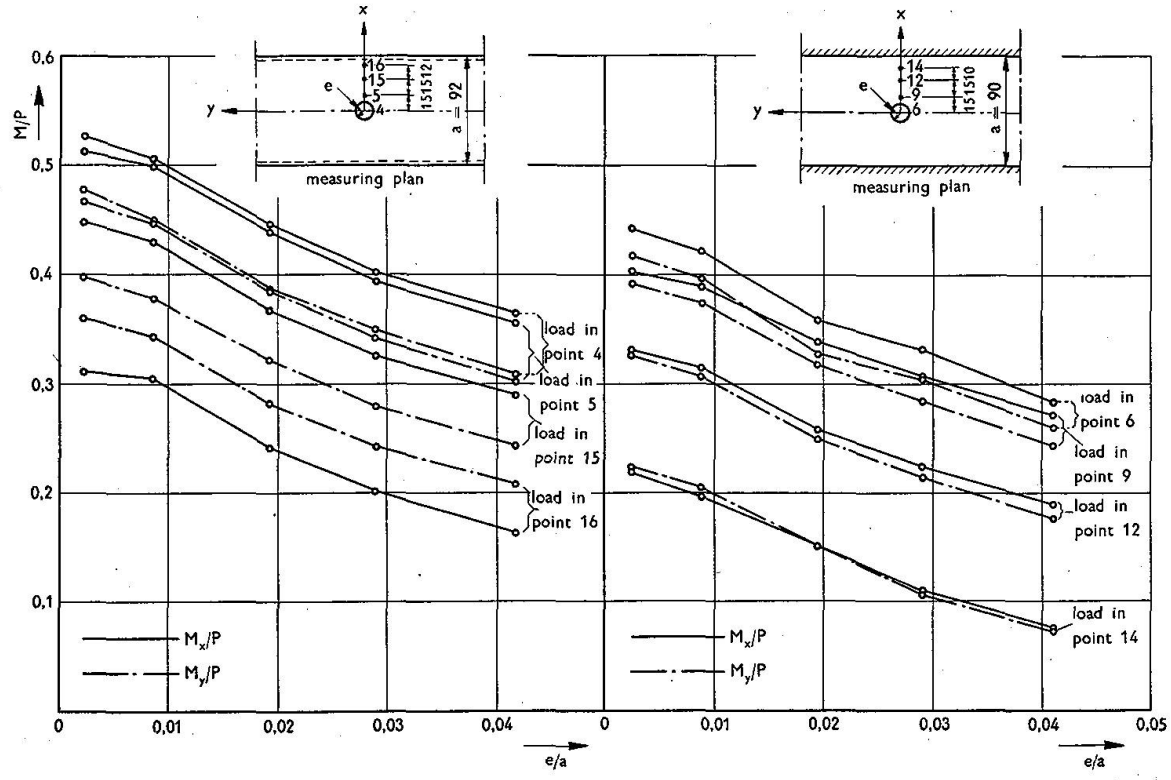

Fig. 4. The bending moments below the load as a function of the concentration e/a.
Load in points 4, 5, 15 and 16 of the central part of the simply supported slab (case *a*). Intermediate layer: cardboard.
Load in points 6, 9, 12 and 14 of the central part of the clamped slab (case *e*). Intermediate layer: cardboard.

The bending moment diagrams have all the same shape (nearly straight and with the same slope), only the level is different.

For the simply supported slab there is a constant difference between the bending moments M_x and M_y at a point, which is nearly the same for the points 4,5 and 15 (M_x always being bigger than M_y). An exception is given by point 16, probably by disturbances from the edge, which is very near. For the clamped slab the conclusions are similar. The level of the diagrams is lowered here by the clamping along the edges. The differences between M_x and M_y are smaller here.

2. *The sphere of influence of the concentration*

For concentrations $e/a = 0{,}0024$ to $e/a = 0{,}0411$ no noticeable influence was found outside an area with a radius of 5 cm (about $\frac{1}{18}$ of the span) around the centre of gravity of the load.

3. *The influence of the intermediate layer*

The bending moments below the load for various concentrations with 3 mm cardboard or rubber and without an intermediate layer are given in fig. 5 for

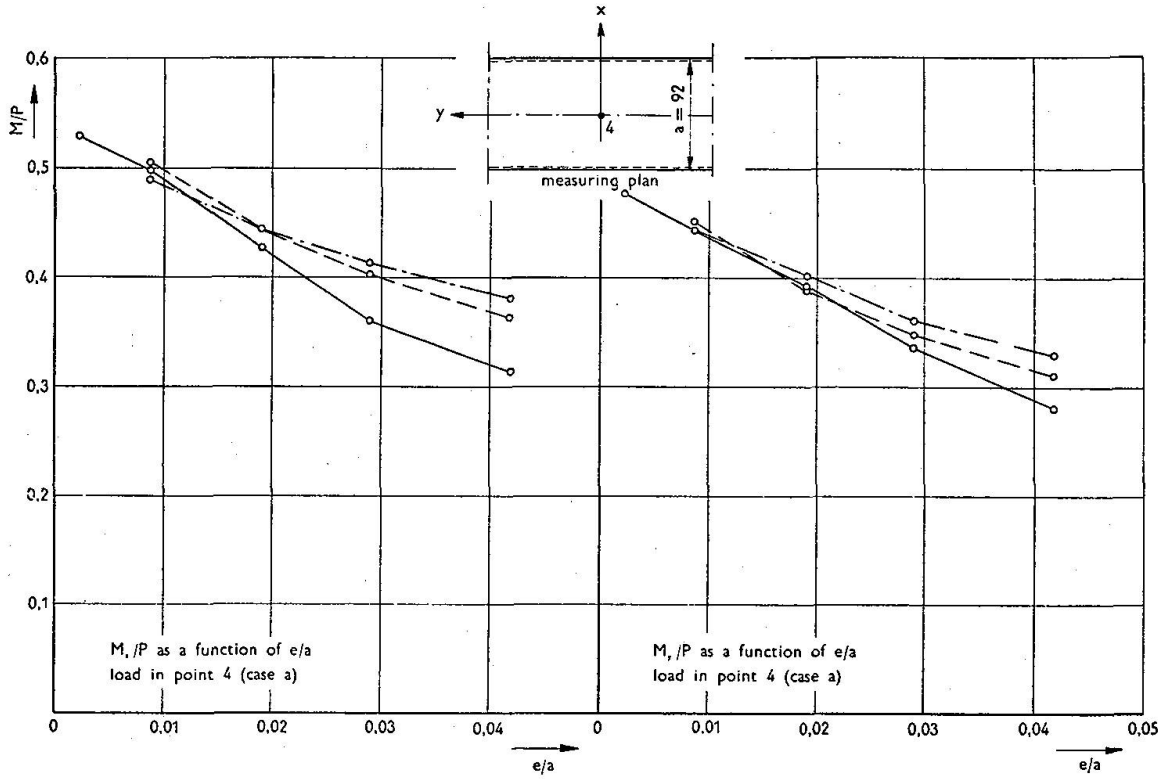

Fig. 5. The influence of different intermediate layers on the moments M_x/P and M_y/P below the load for various concentrations.

Intermediate layer: none ————————
3 m. m. cardboard — — — — — —
3 m. m. rubber — · — · — · —

the simply supported slab when the load is placed in the middle of the span. For the clamped slab the results were similar. With cardboard generally an average value was obtained.

This however is no proof that the load is equally distributed over the contact-area. For the following measurements cardboard was used, also for technical reasons.

4. The distribution of the bending moments in the slab

In the fig. 6 and 7 the derived bending moments are plotted. For every section the point of the extreme moment indicates the point where the load was placed (with an exception for the bending moments along the clamped edge). The load diameter was $D = 1{,}6$ cm (see 2), the intermediate layer was cardboard (see 3). For other diameters the bending moments below the load may be obtained from fig. 4; the bending moments for the other points are practically independent of the concentrations used. The shape of the moment diagrams in the neighbourhood of the extreme values is for all the cases, shown in fig. 6 and 7, nearly the same.

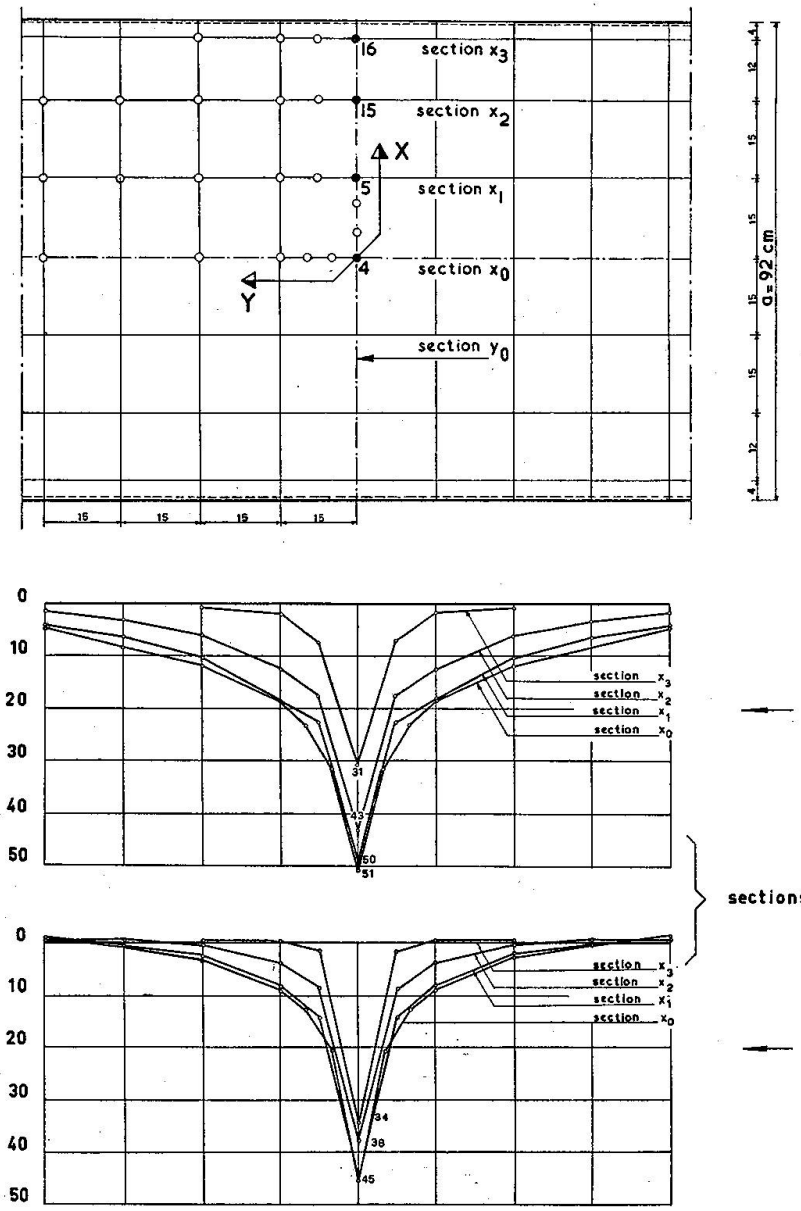

Fig. 6. Bending moment diagrams derived from measurements on the central part of the simply supported slab (case a).

M_x/P and M_y/P

in section x_0: load in point 4
in section x_1: load in point 5
in section x_2: load in point 15
in section x_3: load in point 16
in section y_0: load resp. in point 4, 5, 15, 16.

Loaddiameter $D = 1{,}6$ cm $\left(\frac{e}{a} = 0{,}0087\right)$, intermediate layer: cardboard.

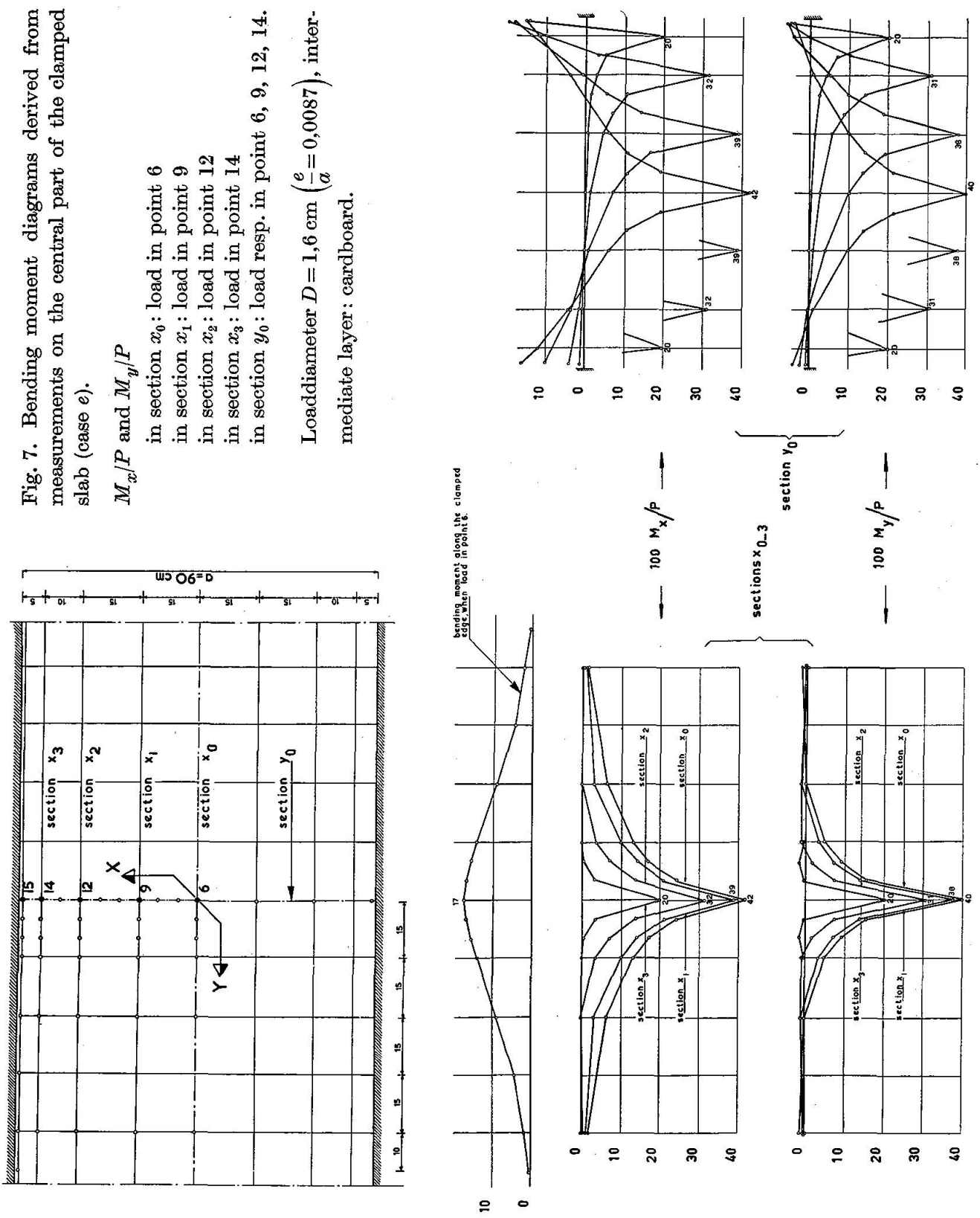

Fig. 7. Bending moment diagrams derived from measurements on the central part of the clamped slab (case e).

M_x/P and M_y/P

in section x_0: load in point 6
in section x_1: load in point 9
in section x_2: load in point 12
in section x_3: load in point 14
in section y_0: load resp. in point 6, 9, 12, 14.

Loaddiameter $D = 1{,}6$ cm $\left(\frac{e}{a} = 0{,}0087\right)$, intermediate layer: cardboard.

The influence of the boundary conditions on the extreme bending moments in the middle part of the span is relatively small (compare fig. 6 and 7). These extreme bending moments decrease only slightly in the beginning when the load moves from the centre towards the edges.

5. The accuracy of the measurements

The results of repeated measurements practically always agreed very well.

An investigation on the accuracy of the measurements showed that the percentage standard error in the value M/P below the concentrated load, placed in the centre of the clamped slab, amounts to 5%. Outside the immediate neighbourhood of the load the absolute standard error is much smaller viz. 0,002 to 0,004.

6. Interpretation of the results

On account of the great width of the slab the moment diagrams for the x-sections may also be considered as influence-lines. For the simply supported slab moreover, Maxwell's law of reciprocity applies, for the bending moments, as can be easily verified from the test results, so that for the central part of this slab the moment diagrams in the y-section are also influence lines.

The values of the bending moments given in the graphs may be converted for a material with an other Poisson's ratio $\bar{\nu}$ (for example concrete $\bar{\nu}=\frac{1}{6}$) with the aid of the following formulæ

$$M_x^{\bar{\nu}} = \frac{(1-\nu\bar{\nu})\,M_x^{\nu}+(\bar{\nu}-\nu)\,M_y^{\nu}}{1-\nu^2}$$

and

$$M_y^{\bar{\nu}} = \frac{(1-\nu\bar{\nu})\,M_y^{\nu}+(\bar{\nu}-\nu)\,M_x^{\nu}}{1-\nu^2}$$

where M_x^{ν} and M_y^{ν} are the values calculated from the measured strains and ν is Poisson's ratio of the material of the model (i.c. $\nu=0{,}3$).

7. Comparison of the test results with the results of the theory

As the theoretical solutions are the simplest for the infinitely wide slabs, with which the central parts of the slabs considered up to now can be compared, the test results from these parts are compared in some detail with the results of the theory.

a) The simply supported slab

Investigated were:

1. The distribution of the bending moments outside of the neighbourhood of the load.
2. The bending moments below the load.
3. The statical equilibrium in a section.

Referring to point 1

As a solution for the differential equation

$$\frac{\partial^4 w}{\partial x^4} + 2\frac{\partial^4 w}{\partial x^2 \partial y^2} + \frac{\partial^4 w}{\partial y^4} = \frac{p}{K},$$

which governs the elementary theory of plates, the following formula is known for the bending moments at the point (x, y) caused by a concentrated load at the point $(-v, 0)$ (fig. 8) (lit. 4).

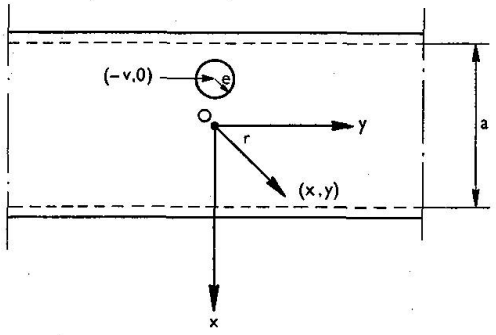

Fig. 8.

$$\left.\begin{matrix} M_x/P \\ M_y/P \end{matrix}\right\} = \frac{1+\nu}{8\pi} \ln \frac{A}{B} \pm \frac{(1-\nu)}{8a} y \sinh \frac{\pi y}{a} \left(\frac{1}{B} - \frac{1}{A}\right)$$

in which

$$A = \cosh \frac{\pi y}{a} + \cos \frac{\pi (x-v)}{a}$$

and

$$B = \cosh \frac{\pi y}{a} - \cos \frac{\pi (x+v)}{a}$$

In fig. 9 the results of this comparison are given for the moment M_x in the section x_0. The agreement between experiment and theory is proved to be very good. For M_x in the section y_0 and M_y in the sections x_0 and y_0 the agreement was similar.

The values obtained in the experiments with a ball are plotted in fig. 9 to approach as nearly as possible the case of a load concentrated at a simple point.

Referring to point 2

The elementary theory of plates does not take in account the thickness of the plate and therefore does not apply to the immediate neighbourhood of a strongly concentrated load.

According to WESTERGAARD (lit. 4) the thickness of the slab may be taken into account in the following way; the total load P, which acts on a circular area with a radius e is assumed to be distributed over an area with a radius e',

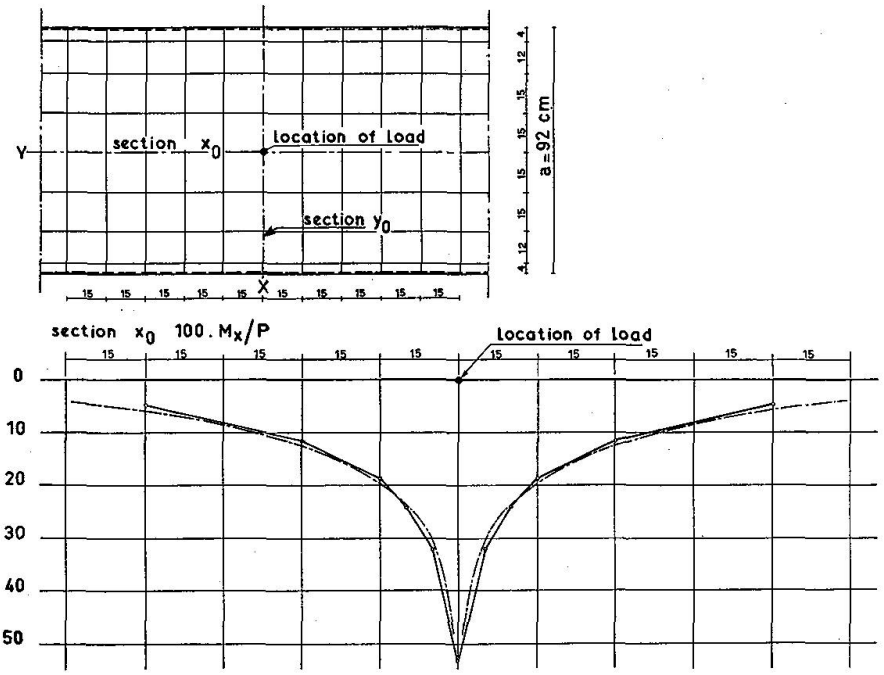

Fig. 9. Bending moment diagram from test results compared with these according to the elementary theory of plates.

Concentrated load (ball) in the centre of the simply supported slab (case *a*).

— · — · — · — · According to the elementary theory of plates.

——————— According to test results.

which is determined in such a way that the stresses computed according to the elementary theory of plates are equal to the exact stresses. For values of $D = 2e < 3{,}45h$ the fictive radius e' may be computed with the formula $e' = \sqrt{1{,}6e^2 + h^2} - 0{,}675h$. For values of $D > 3{,}45h$, it may be assumed that $e' = e$. The bending moments below the load are then computed with the following formula (see also fig. 8)

$$\left.\begin{matrix} M_x/P \\ M_y/P \end{matrix}\right\} = \frac{1+\nu}{4\pi}\left\{\ln\left(\frac{2a}{\pi e'}\cos\frac{\pi v}{a}\right) + \frac{1}{2}\right\} \pm \frac{(1-\nu)}{8\pi}$$

For locations of the load at some points of the span the results of the theory of WESTERGAARD are compared with the test results for various concentrations of the load. The agreement proved to be good (fig. 10).

For a load located at the centre of the span the bending moments M_x, calculated according to the elementary theory of plates are also plotted in fig. 10. The deviation of the results of the elementary theory are for this thin slab only of importance for concentrations $e/a < 0{,}01$. To show the influence of the thickness the values of M_x/P according to WESTERGAARD are also plotted for ratio's $h/a = {}^1/_{30}$ and ${}^1/_{15}$.

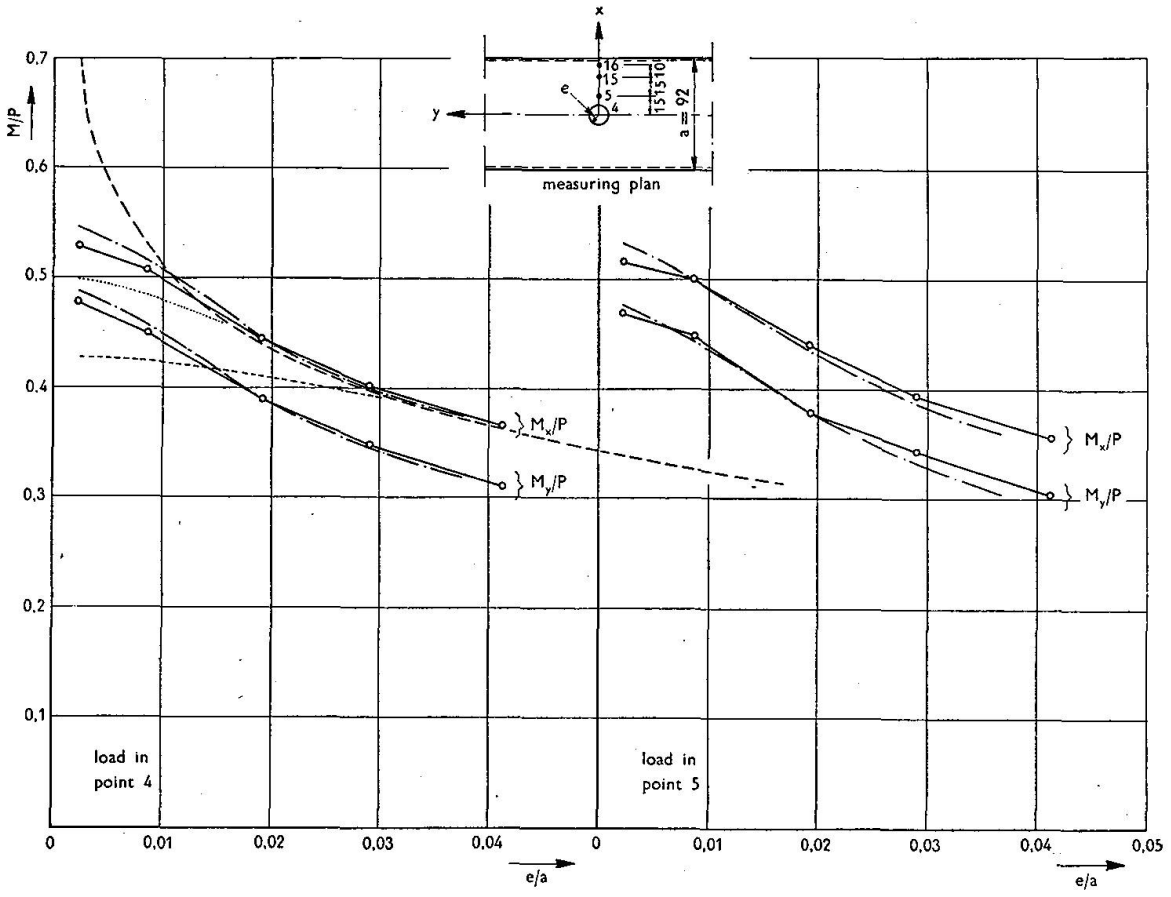

Fig. 10. Comparison of test results with the results of the elementary theory of plates and with the theory of Westergaard. The bending moments under the load are plotted as a function of the concentration e/a when the load is located in some points of the span in the central part of the simply supported slab. Intermediate layer cardboard.

———————— according to test results.
— — — — — — — according to the elementary theory of plates ($\nu = 0{,}3$).
— · — · — · — · according to Westergaard ($\nu = 0{,}3$).
. . . . . dito for a ratio $h/a = 1/30$ ($\nu = 0{,}3$).
---------- dito for a ratio $h/a = 1/15$ ($\nu = 0{,}3$).

Referring to point 3

A good check on the test results is obtained by determining the total bending moment in a section. For a concentrated load at the middle of the span this total moment in the section x_0 must be $\frac{1}{4} P l$. If the load is distributed over an area with finite dimensions, in this case $D = 1{,}6$ cm, this moment will be somewhat smaller. The derived moment diagram is not complete, because it only extends over a limited width. The remaining parts have been supplemented by the results of the theory. In this way no large error can be made because the values concerned are small. The total bending moment obtained in this way differs by less than 1% from the value computed by the direct method given above.

The following verifications were also made for the clamped slab:

1. The stress distribution outside the neighbourhood of the load.
2. The stress distribution below the load.
3. The statical equilibrium.

Referring to point 1

The bending moments in the middle part of the span are reduced by the bending moments along the clamped edge, compared with those of the simply supported slab.

For the concentrations used, the clamping moments are not effectively influenced by the size of the loaded area. The reductions of the moments in the middle part therefore also will be independent of this size. Formulas herefor are known from the literature (4).

With the aid of these formulas the moments in the middle part of the span have been computed and then compared with those determined from the measurements. The agreement proved also to be very good.

For checking the clamping moments it is difficult to determine the exact location of the clamping (rounded corners!). Moreover the nearest strain-gauge was pasted at some distance from the corner so that the moment at the clamping point had to be determined by a small extrapolation. The maximum clamping derived in this way from the measurements amounts to $M_x/P = 0{,}172$. This is in good agreement with the theoretical value of $M_x/P = 0{,}169$ (obtained from lit. 1). The other values of the clamping moment diagram were also in very good agreement with the theoretical values.

Referring to point 2

The bending moments below the concentrated load, when the load is placed at the centre of the span, have been computed from the corresponding bending moments in the simply supported slab by a reduction in the way mentioned above. The results were in very good agreement with the values obtained from the measurements.

Referring to point 3

The checking of the statical equilibrium provided also a satisfactory agreement between theory and experiment.

B. The end-parts of the slabs (near the short sides)

For the central parts of the slabs, as already described, first the influence of the magnitude of the concentration of the load on the bending moments has been investigated. The sphere of influence was proved to be very limited. The investigation on this influence was thereupon concluded.

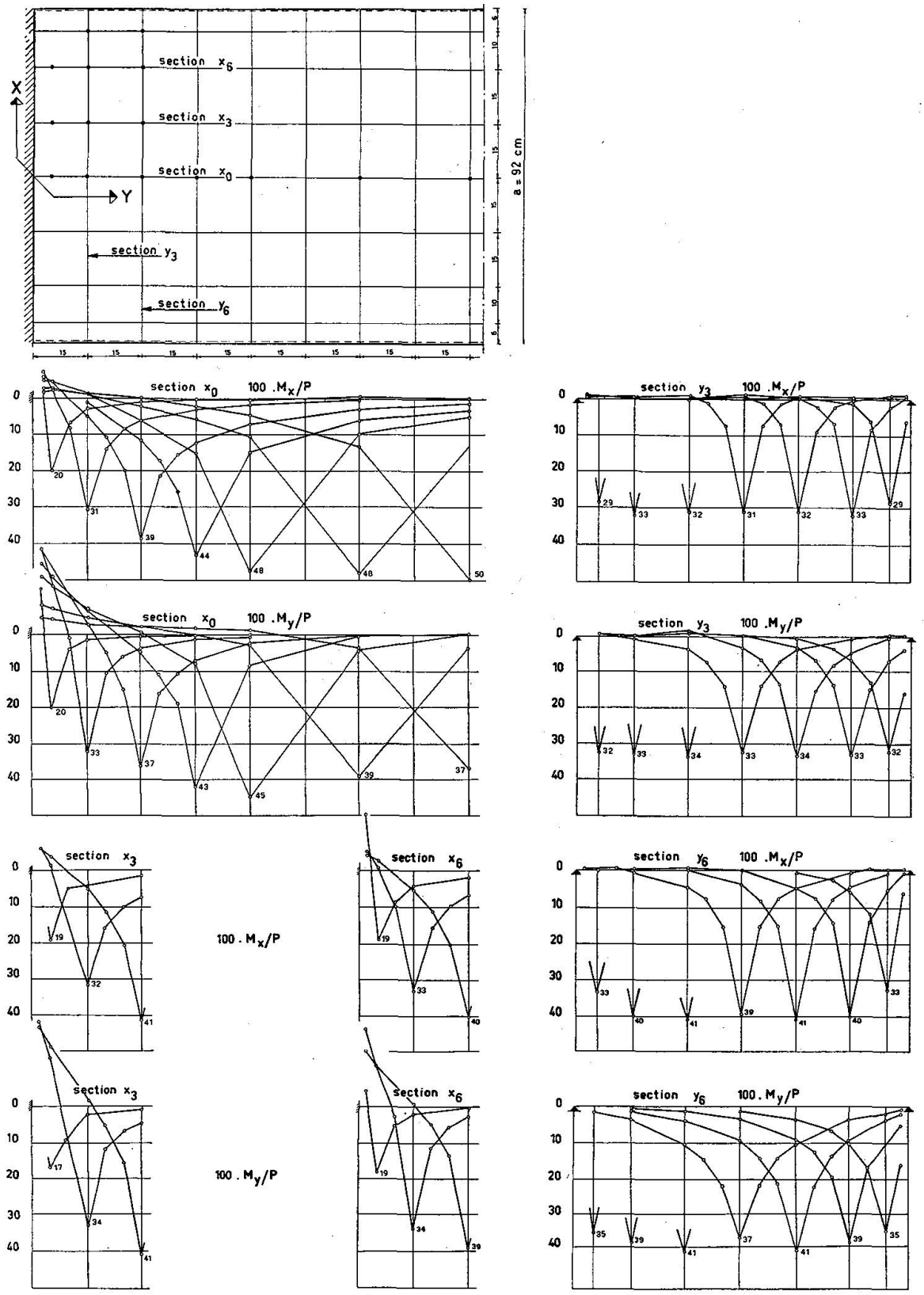

Fig. 11. Bending moment diagrams derived from measurements: Case *b* (see fig. 3). Loaddiameter $D = 1{,}6$ cm ($e/a = 0{,}0087$), intermediate layer: cardboard.
· = locations of the load.
In the diagrams the locations of the load are always indicated by the biggest moments.

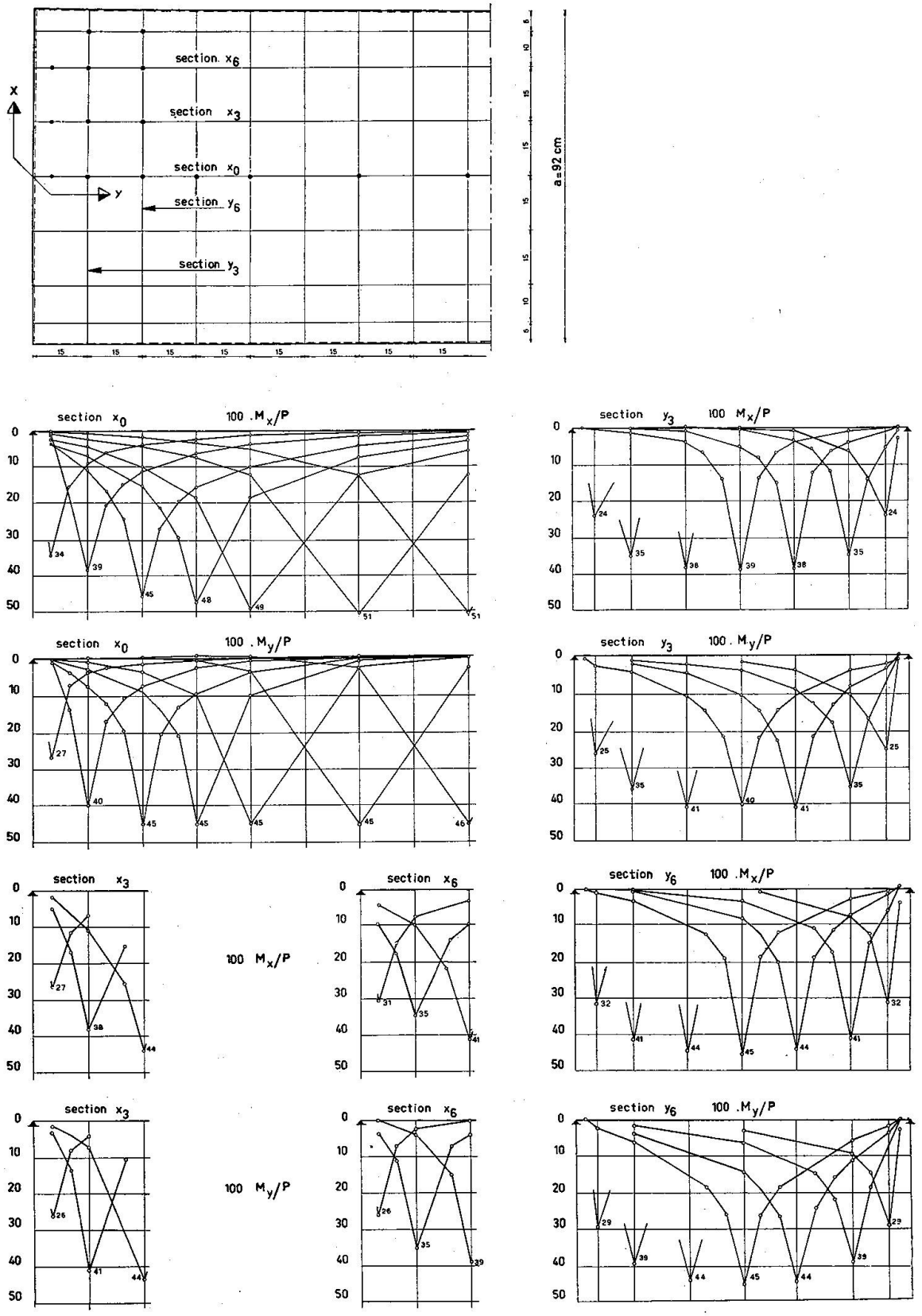

Fig. 12. Bending moment diagrams derived from measurements: Case c (see fig. 3). Loaddiameter $D = 1{,}6$ cm ($e/a = 0{,}0087$), intermediate layer: cardboard.
· = locations of the load.
In the diagrams the locations of the load are always indicated by the biggest moments.

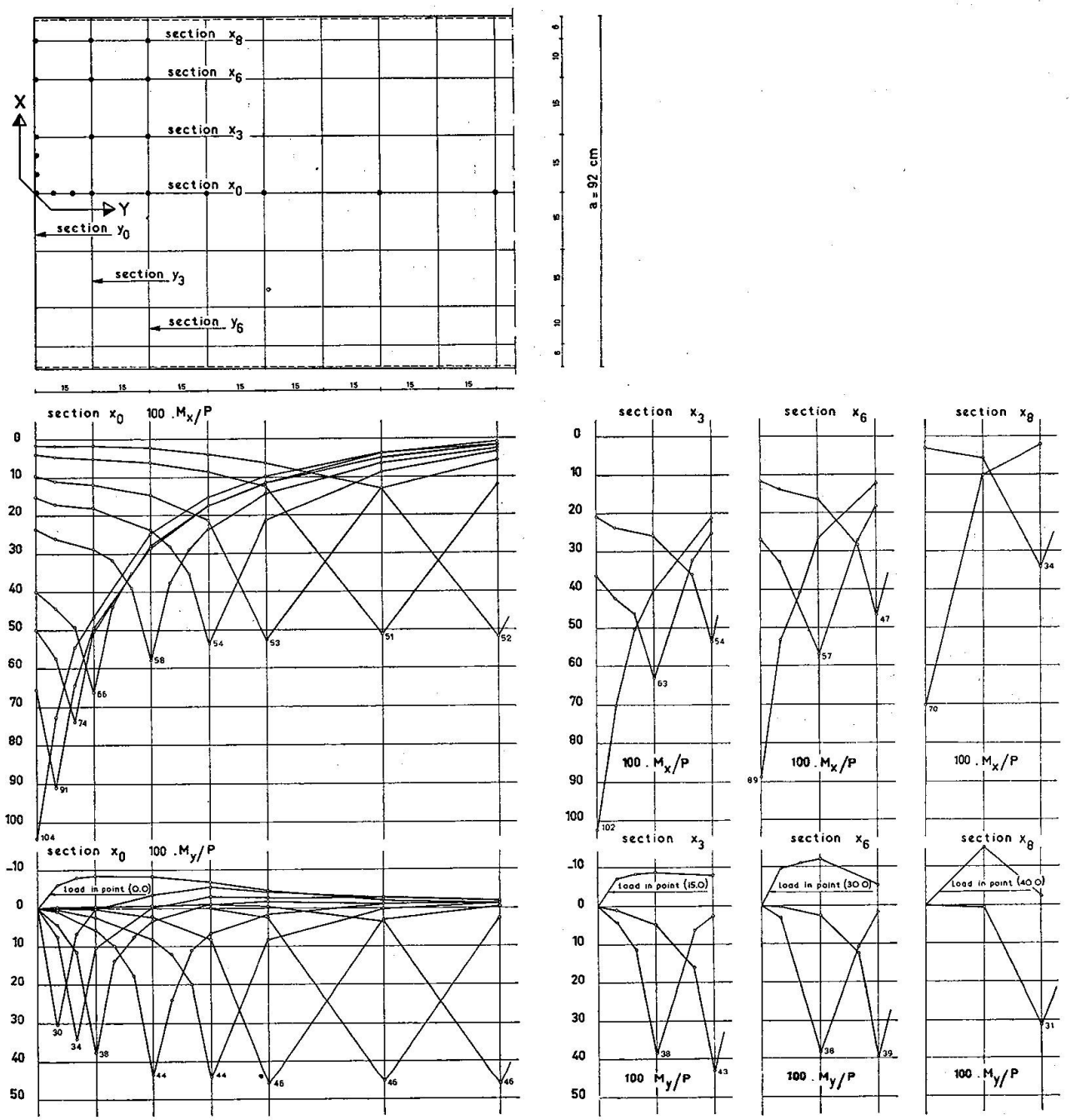

Fig. 13a. Bending moment diagrams derived from measurements: Case d (see fig. 3). Loaddiameter $D = 1{,}6$ cm ($e/a = 0{,}0087$), intermediate layer: cardboard.
· = locations of the load.
In the diagrams the locations of the load are always indicated by the biggest moments.

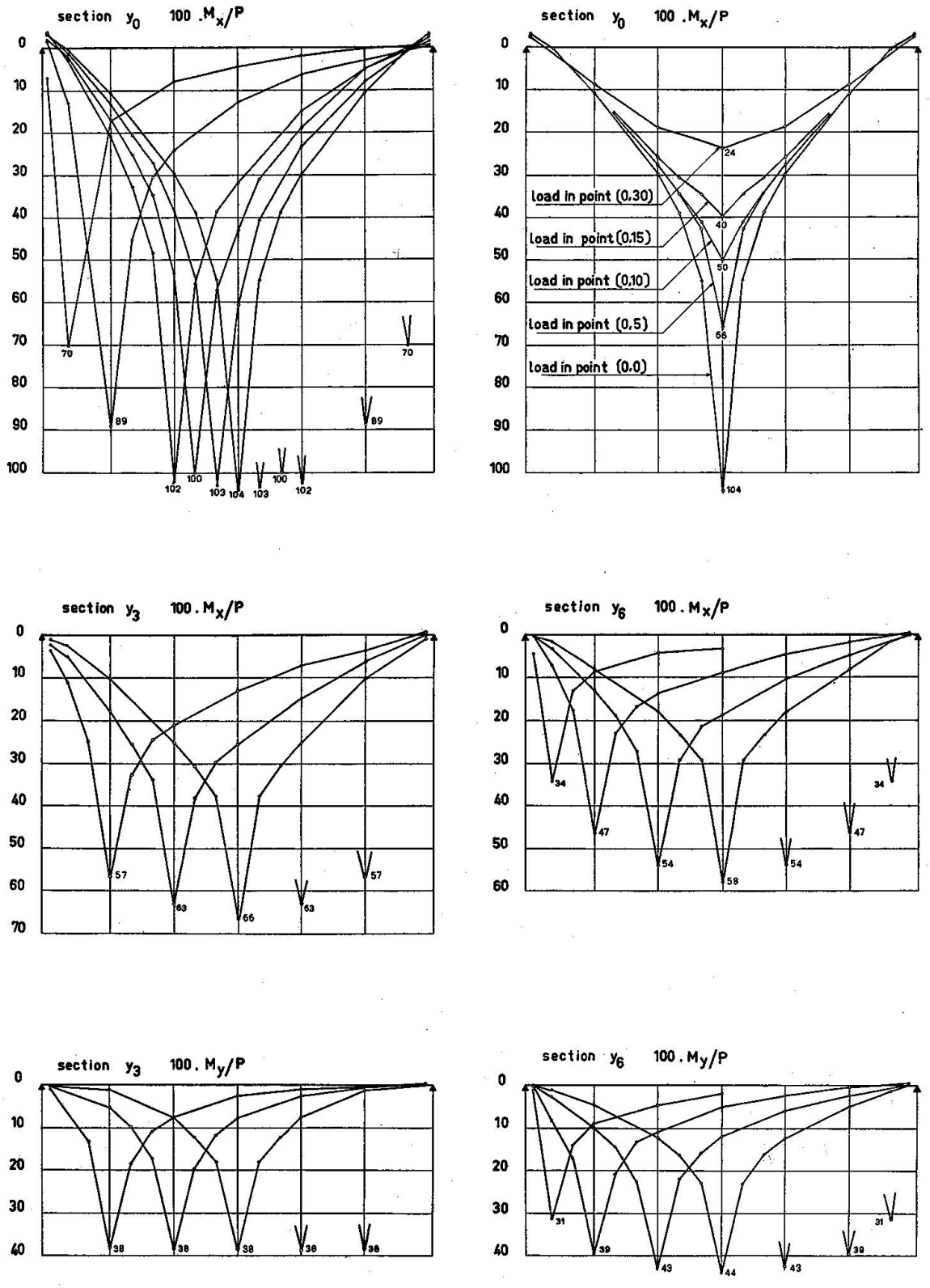

Fig. 13b. Bending moments along the free edge, when the load is placed in section x_0, respectively on a distance of 0, 5, 10, 15 and 30 cm from the edge.

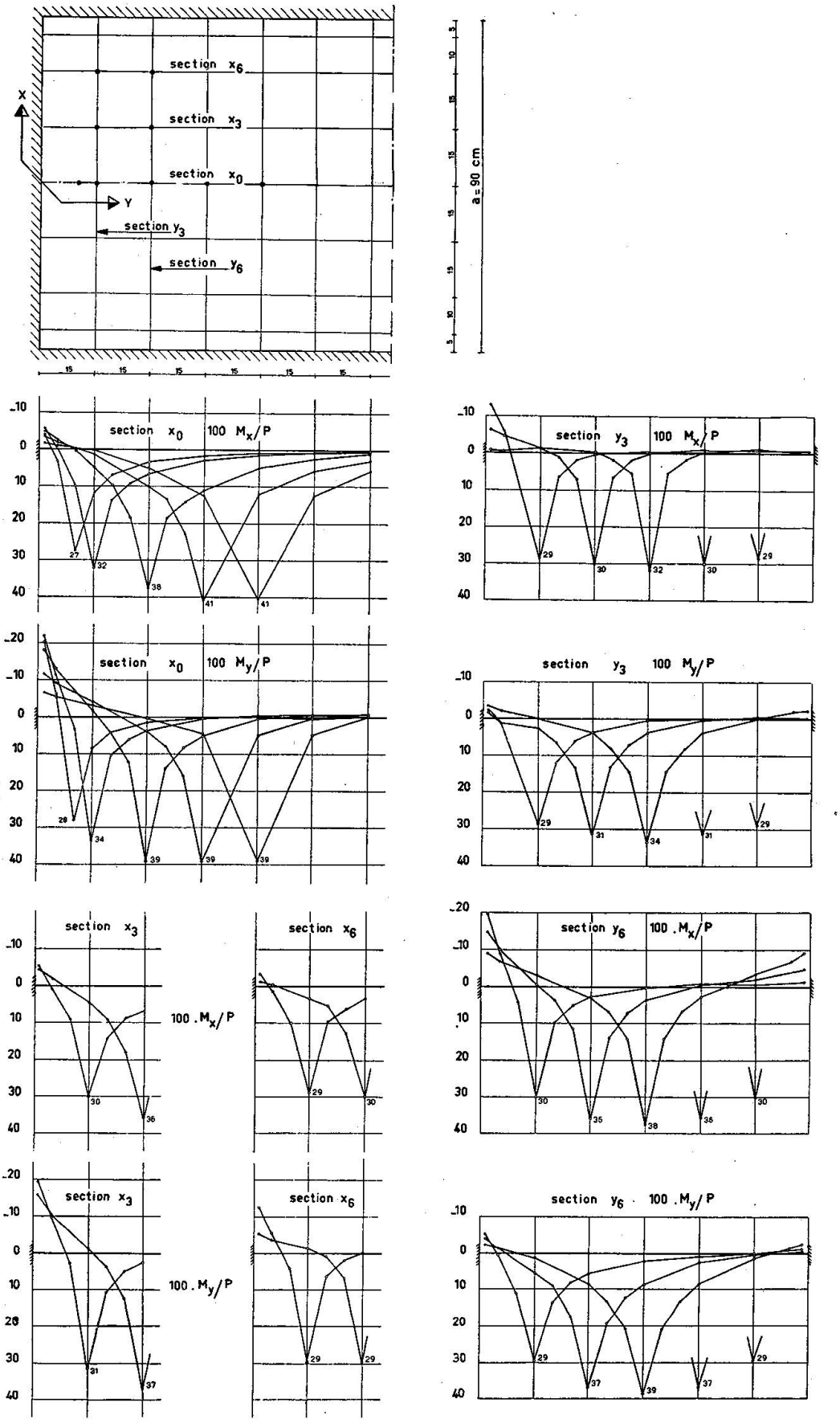

Fig. 14. Bending moment diagrams derived from measurements: Case *f* (see fig. 3). Loaddiameter $D = 1{,}6$ cm ($e/a = 0{,}0087$), intermediate layer: cardboard.
· = locations of the load.

In the diagrams the locations of the load are always indicated by the biggest moments.

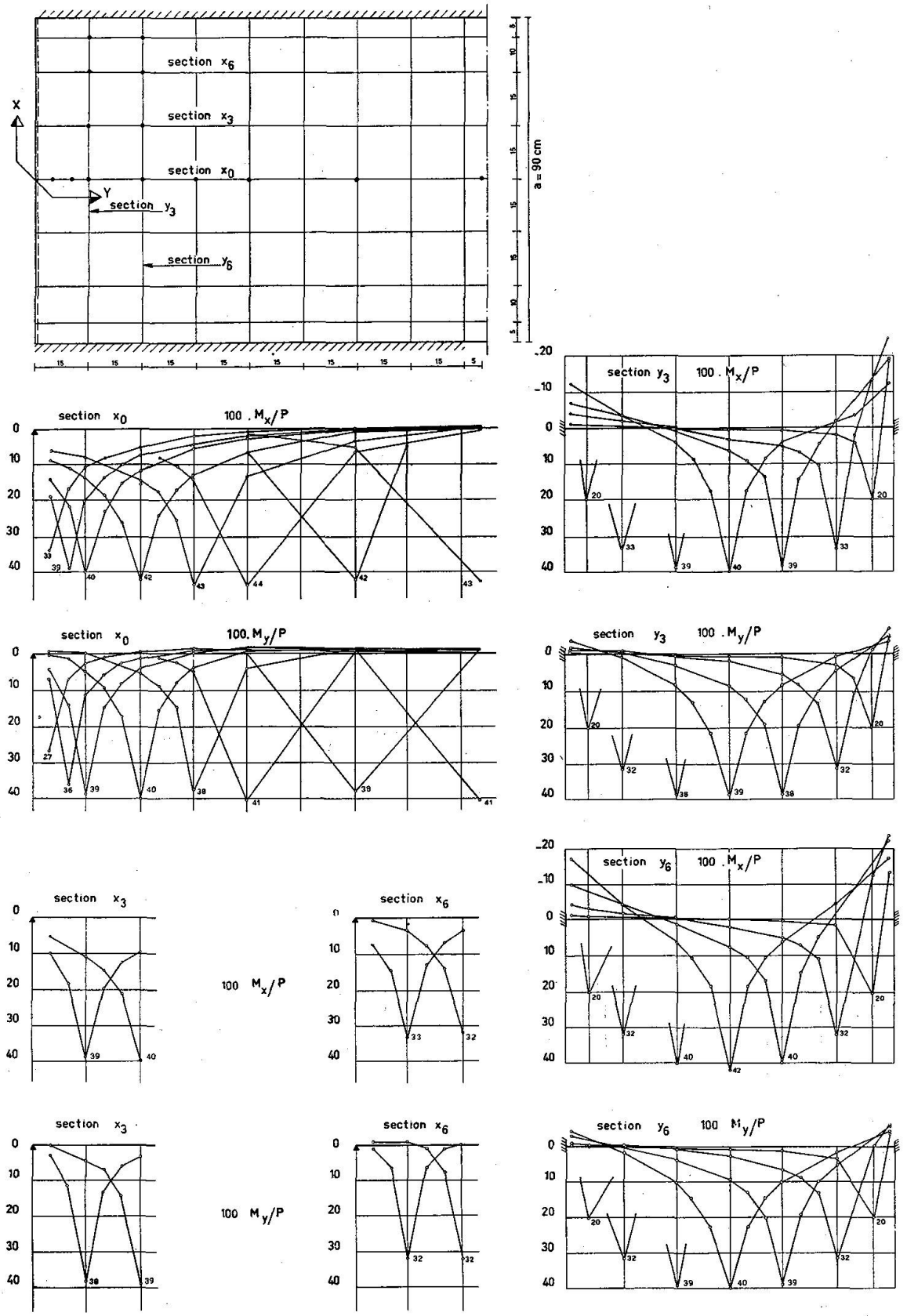

Fig. 15. Bending moment diagrams derived from measurements: Case *g* (see fig. 3). Loaddiameter $D = 1{,}6$ cm ($e/a = 0{,}0087$), intermediate layer: cardboard.
· = location of the load.
In the diagrams the locations of the load are always indicated by the biggest moments.

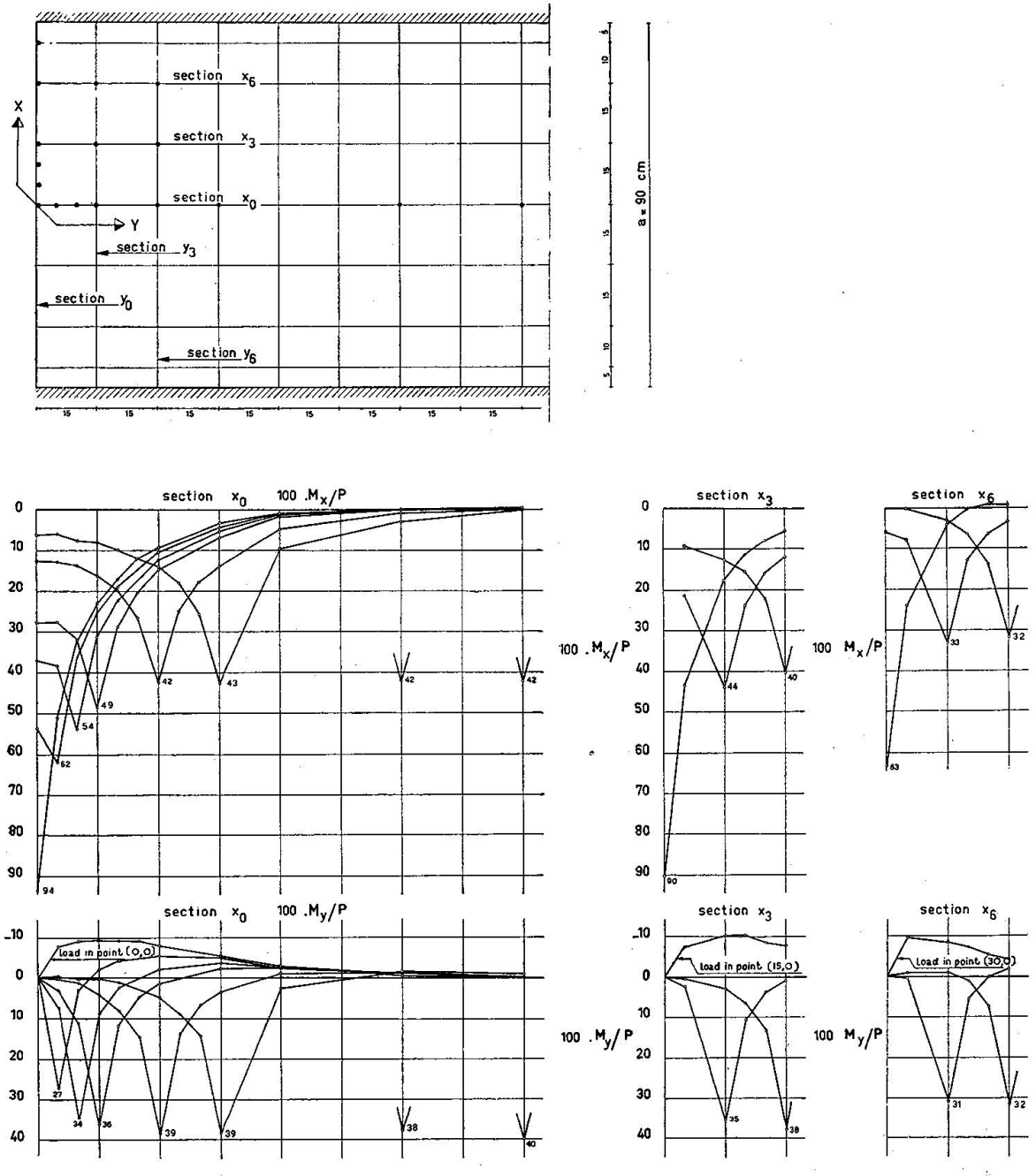

Fig. 16a. Bending moment diagrams derived from measurements: Case h (see fig. 3). Loaddiameter $D = 1{,}6$ cm ($e/a = 0{,}0087$), intermediate layer: cardboard.
· = location of the load.
In the diagrams the locations of the load are always indicated by the biggest moments.

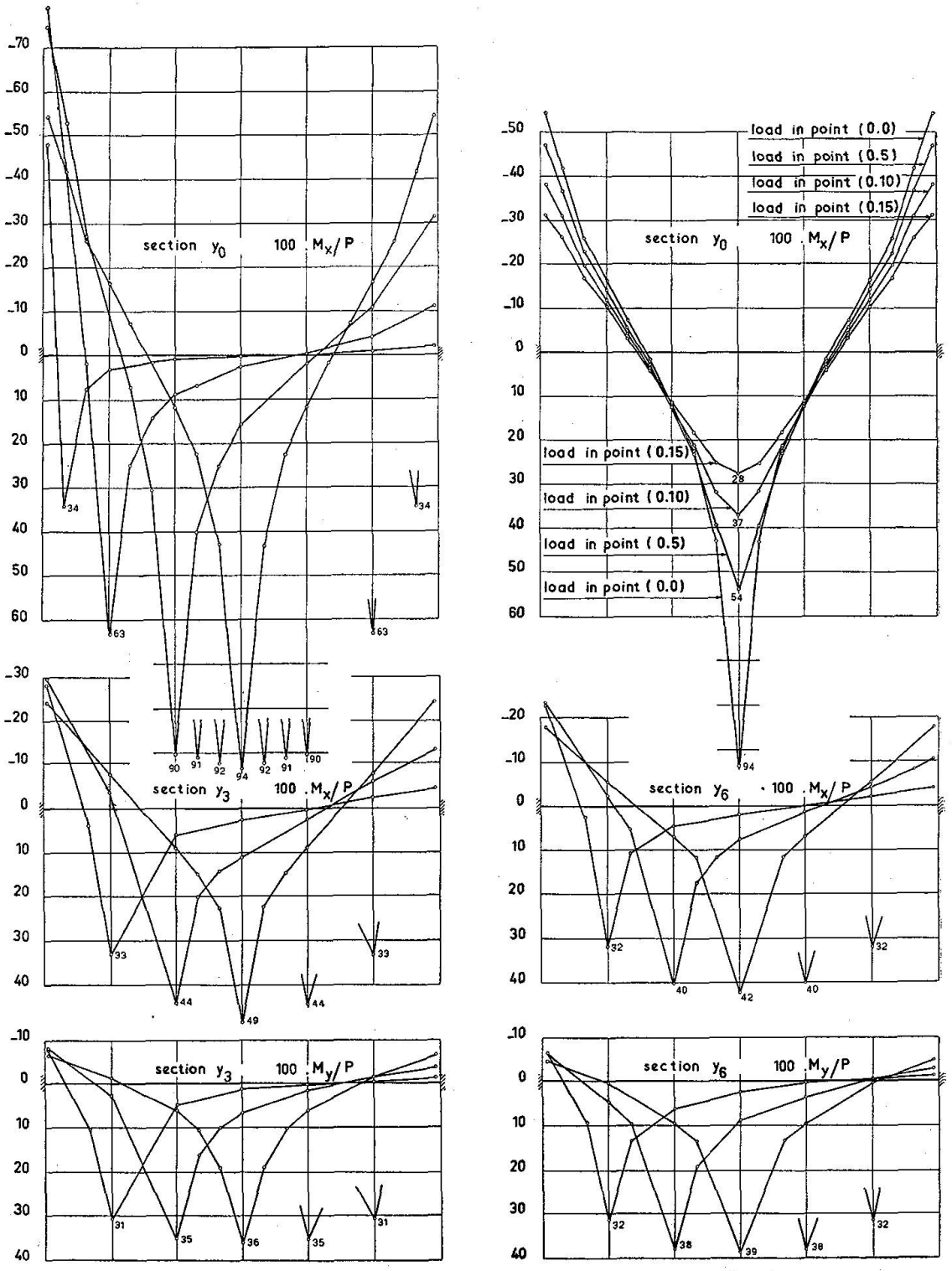

Fig. 16b. Bending moments along the free edge, when the load is placed in section x_0, respectively on a distance of 0, 5, 10 and 15 cm from the edge.

For the end parts only the distribution of the bending moments for various locations of the load was investigated. Only one load-diameter viz. $D = 1{,}6$ cm ($e/a = 0{,}0087$) was used. The intermediate layer was cardboard.

The test results are given in figs. 11—16.

The load is always placed at the marked points, to which refer the curves that give the maximum moments there.

In fig. 17 are given for the various cases viz. *b*, *c*, *f* and *g* (from fig. 3) the curves of the maximum moments (the envelopes of the moment diagrams in the sections).

Some comments on these moment diagrams are listed below.

1. The shape of the moment diagrams in the neighbourhood of the maximum values is for most cases nearly the same. Only in the immediate neighbourhood of an edge are there deviations.
2. The influence of the boundary conditions on the maximum bending moments, outside the immediate neighbourhood of the edges, is relatively small.
3. These maximum bending moments decrease only slightly in the beginning when the load moves from the centre towards the supported or clamped edges.
4. For the simply supported slabs the moments derived from the measurements conform to the law of reciprocity. These moment-diagrams are therefore also influence lines.
5. The moment diagrams in section y_0 for case (*h*) (fig. 3) are very steep (fig. 16). Comparison to case (*d*) (fig. 13) shows that the positive bending moments in the middle of the free edge are only slightly reduced by the very big clamping moments, viz. from $1{,}042\,P$ (long sides simply supported) to $0{,}935\,P$ (long sides clamped).
6. The bending moments in the centre of the free edge are for the same concentration for case (*d*) and case (*h*) somewhat more than twice the bending moments in the centre of the span for cases (*a*) and (*e*) respectively

$$\text{Case } a\text{: } M_x/P = 0{,}507, \text{ case } d\text{: } M_x/P = 1{,}042$$

$$\text{ratio } M_d/M_a = \frac{1{,}042}{0{,}507} = 2{,}05.$$

$$\text{Case } e\text{: } M_x/P = 0{,}422, \text{ case } h\text{: } M_x/P = 0{,}935$$

$$\text{ratio } M_h/M_e = \frac{0{,}935}{0{,}422} = 2{,}20.$$

7. The influence of the free edge is limited to a narrow zone of about $\frac{1}{3}\,l$ (case *d* and *h*, fig. 13 and 16).

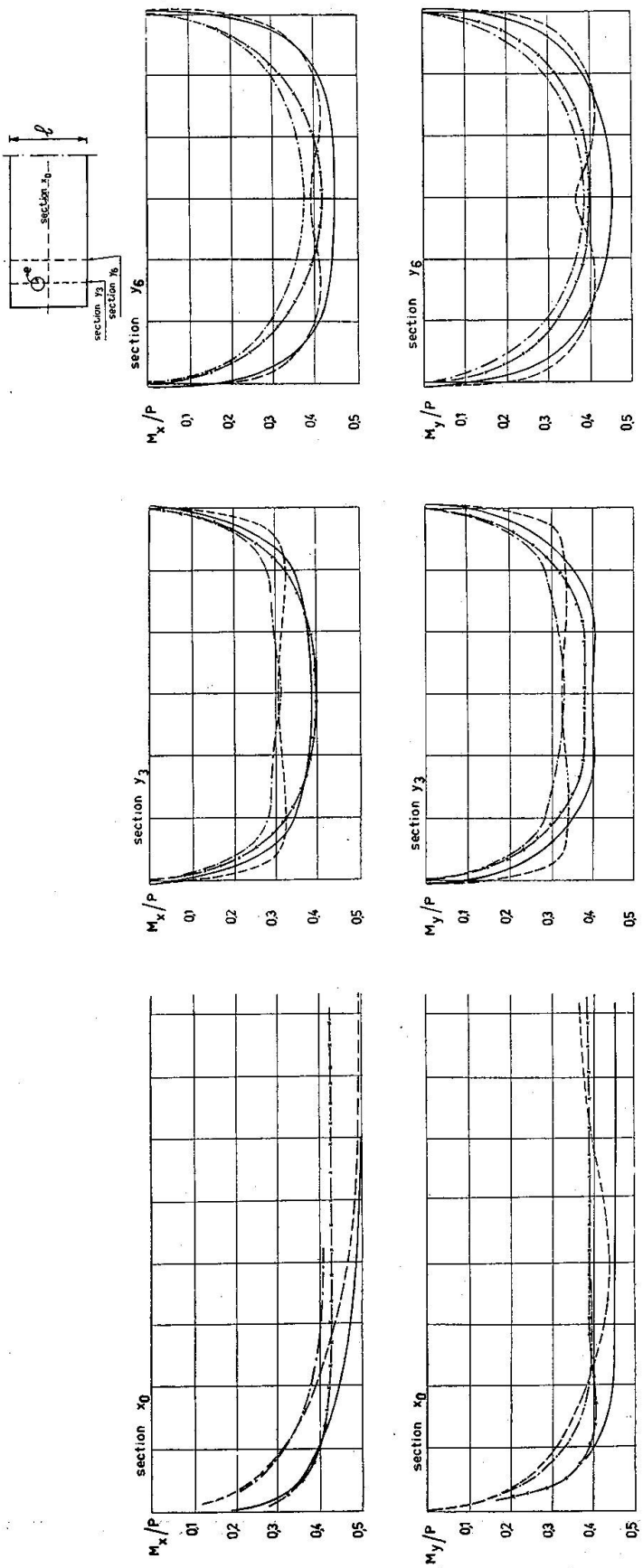

Fig. 17. Diagrams of extreme bending moments M_x/P and M_y/P derived from measurements, dependent on the boundary conditions of the slab.

Dimensions of slab $b \sim 6\,l$. Load concentration $e/l = 0{,}0087$.

——— Short side simply supported, long sides simply supported: case c (see fig. 3).
– – – – Short side clamped, long sides simply supported: case b (see fig. 3).
—·—·—· Short side clamped, long sides clamped: case f (see fig. 3).
—×—×— Short side simply supported, long sides clamped: case g (see fig. 3).

The interpretation of the results

For slabs with simply supported or clamped edges the bending moments may be converted for a material with another Poisson's ratio ν by using the formulas already given for the infinitely wide slabs. For slabs with a free edge this is not permissible because the quantity ν occurs in the boundary conditions, which are necessary to solve the differential equation of the slab. For these cases the given moment diagrams may be used. For a material with a smaller value of ν (e. g. for concrete $\nu = {}^1/_6$) the discrepancies will be small and on the safe side.

Conclusions

All measured bending moments may be considered as experimental solutions of the theory of elasticity. Verification of the measurements with theoretical results showed:

a) Outside the immediate neighbourhood of the load there was a good agreement between the experiments and the elementary theory of plates.
b) For the bending moments under the load, the correction on this theory by WESTERGAARD was in good agreement with the experiments.

Acknowledgements

This investigation has been carried out by the Section for Reinforced Concrete and Steel Constructions T.N.O. at the suggestion of and in cooperation with the Board of Bridges of the Department of Public Works (Rijkswaterstaat).

The authors desire to thank the chairman of the above-mentioned Section, Prof. Ir. C. G. J. VREEDENBURGH of the Technological University of Delft, the Netherlands, for his help and advice.

Furthermore the following persons have worked on this investigation: Ir. J. G. BAAS, former T.N.O. engineer; W. J. VAN DEN BOOGAARD and J. S. KUYPER, technical assistants T.N.O.; and several students of the Technological University of Delft, the Netherlands.

Literature

1. A. PUCHER: Einflussfelder elastischer Platten, Wien 1951.
2. A. NADAÏ: Die elastischen Platten, Berlin 1925.
3. S. P. TIMOSHENKO: Theory of plates and shells. New York 1940.
4. H. M. WESTERGAARD: Computations of stresses in bridge slabs due to wheel loads, Public Roads, vol. 11, no. 1, March 1930.

Summary

To obtain information about the stress-distribution in reinforced concrete slabs, subjected to concentrated loads, experiments have been conducted on a steel model. The strains were measured with electrical resistance strain-gauges.

The research program has consisted of:

1. Investigation of the influence of the size of the loaded surface (the concentration of the load) on the bending moments in the slab.
2. Investigation of the stress-distribution in the slab as a function of the boundary-conditions and the location of the load.

The results, given in graphs, are discussed and in some cases compared with the results of the theory.

Résumé

Des essais ont été effectués sur un modèle en acier, afin d'obtenir des informations sur la répartition des contraintes dans les dalles en béton armé soumises à des charges concentrées. Les contraintes ont été mesurées à l'aide d'extensomètres à résistance électriques.

Le programme de recherches a comporté les deux stades suivants:

1. Etude de l'influence des dimensions de la surface chargée (concentration de la charge) sur les moments fléchissants dans la dalle.
2. Etude de la répartition des contraintes dans la dalle en fonction des conditions des bords et de la localisation de la charge.

Les résultats, publiés sous la forme de graphiques, sont discutés et dans certains cas, comparés avec ceux de la théorie.

Zusammenfassung

An einem Stahl-Modell wurden Versuche durchgeführt, um über die Spannungsverteilung in Eisenbetonplatten, die von Einzellasten beansprucht werden, Aufschluß zu erhalten.

Die Spannungen wurden mit Hilfe elektrischer Widerstands-Spannungsmesser ermittelt.

Das Forschungsprogramm umfaßte:

1. Untersuchung des Einflusses der Größe der belasteten Oberfläche (bei Einzellast) auf die Biegungsmomente in der Platte.
2. Untersuchung über die Spannungsverteilung in der Platte als Funktion der Randbedingungen und der Lage des Angriffspunktes der Einzellast.

Die graphisch dargestellten Resultate werden besprochen und in einzelnen Fällen mit den theoretischen Werten verglichen.